DIMUON PRODUCTION IN A BEAM DUMP DETECTOR BY 400 GeV PROTONS

Paul M. Mockett
Department of Physics, FM-15
University of Washington, Seattle, Washington USA 98195

Abstract: Results from 225,000 dimuon events with mass above 6 GeV obtained in a beam dump detector are presented. The sea quark structure functions are determined from the mass spectrum and are found to be a factor of 1.6±0.3 larger than those obtained from inelastic neutrino scattering. A test of the Drell-Yan model over the Feynman x, x_F, range of -0.2 to 1.0 is made for masses up to 14 GeV. The x_F dependence of the Upsilon family production cross section is given. Also presented is the average P_t of the dimuon pairs versus x_F and the mass. A small increase with mass is indicated, but no significant decrease with x_F is found.

1. Introduction*

The results of the MNTW** collaboration presented in this talk are based on data taken at Fermilab in the spring of 1978. The first data obtained in this experiment were taken at the time of the discovery of the Upsilon family by the CFS group.[1] Confirmation of this meson family was first reported by the MNTW group in D. A. Garelick et al.[2] Approximately 225,000 dimuon pairs with mass above 6 GeV were recorded. These were produced by 400 GeV/c protons on a tungsten target. About 15,000 events in the Upsilon family were contained in this sample.

The experimental technique employed can be characterized as a beam dump detector. The advantages of this device are: (1) a high rate capability of up to 10^{12} protons per pulse; (2) a large overall acceptance of approximately 6% and all Feynman x greater than -0.2; (3) a multi-muon detection capability where three or more muons might be seen, for example, if naked charm or bare bottom mesons were produced in coincidence with the J/ψ or Υ resonances. The detector could also have recorded low mass pairs produced at large P_t had we realized the importance of studying this process at that time.

The disadvantages of the device are: (1) a poor mass resolution of about 7.5%; (2) a contamination from dimuons produced by secondary hadrons in the long target and dump. As an aside we note that an air gap magnet placed downstream of the dump would have enabled this technique to obtain a mass resolution of about 2% at large mass. The Northeastern Group component of this collaboration is proposing to do this in Fermilab Experiment P645.

In this paper we will report on (1) the sea quark structure functions as determined from our dimuon spectrum and K factor; (2) a test of the Drell-Yan model; (3) the Feynman x dependence of the ratio of the Upsilon production to that of the continuum; (4) the average P_t dependence of the dimuon pairs as a function of both Feynman x and dimuon mass.

2. The Detector

Our apparatus is shown in Fig. 1. A 400 GeV/c proton beam is incident from the left and impinges on a 32 cm tungsten target. The target is placed

* This work was supported by the National Science Foundation and the Department of Energy.

** The institutions involved in this collaboration are University of Michigan, Northeastern University, Tufts University, and the University of Washington. The collaborators were S. Childress, D. A. Garelick, P. S. Gauthier, M. J. Glaubman, H. R. Gustafson, L. W. Jones, H. Jonstad, M. J. Longo, M. L. Mallary, P. M. Mockett, J. Moromisato, W. P. Oliver, E. Pothier, T. J. Roberts, J. P. Rutherfoord, S. R. Smith, E. von Goeler, M. R. Whalley, and R. W. Williams.

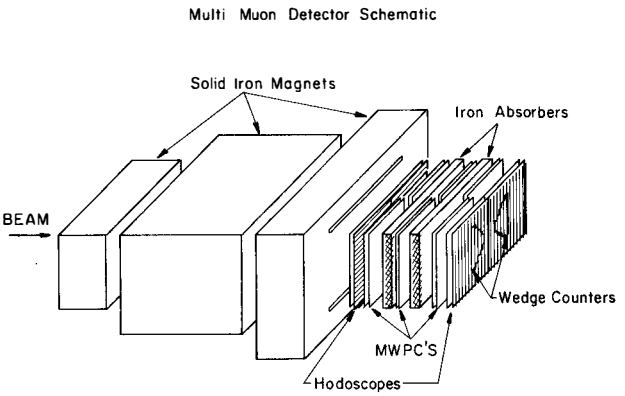

Fig. 1. Beam Dump Detector Schematic. The 400 GeV/c proton beam is incident from the left and impinges on a 32 cm tungsten target. The 5.5m of solid iron magnets have a horizontal field of 2.15T.

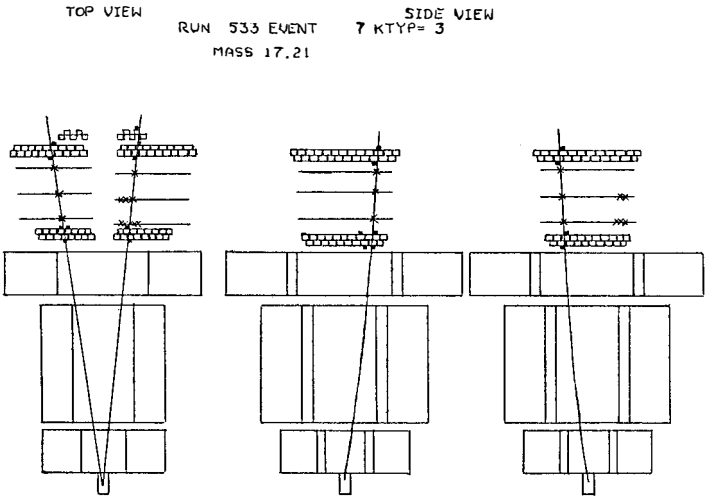

Fig. 2. Typical High Mass Event. The hodoscope and PWC hits of a 17 GeV mass dimuon event are shown along with the reconstructed trajectories.

next to the first dump magnet so that background from pion decays is minimized. The 5.5m of beam dump magnets carry a horizontal field of 2.15T and also serve as the analysis magnets.

Following the iron is the dimuon detector. It is composed of two mirror-image arms whose opening angle can be adjusted for different running conditions. Most of the running was taken with the arms making a minimum angle of 18 mr with respect to the target. Each arm begins with two planes of trigger hodoscopes which give the horizontal and vertical position of muons traversing the magnets. These hodoscopes are followed by 9 planes of proportional wire chambers grouped into three sets. Each set is separated by a 7-inch slab of iron to prevent showers produced near the end of the magnet from penetrating all the planes. Following the proportional wire chambers is another set of horizontal and vertical trigger hodoscopes.

Following these hodoscopes is a final set of vertical hodoscopes which were used to restrict the triggers to the highest mass. These formed a wedge-shaped pattern and were used in the trigger to replace the inner back vertical hodoscopes that they overlapped. The bulk of our high mass data was obtained with this requirement. The fast trigger required hits in the four planes of hodoscopes in each arm. The latched hodoscope hits were then viewed by a matrix logic unit based on the memory chip developed by Brookhaven National Laboratory. This matrix logic imposed a higher momentum cut than was produced by the acceptance of the magnets and hodoscopes, and it required the dimuon trajectories to point back to the target in the non-bend plane. If these requirements were not satisfied the event was aborted. The trigger was very clean and approximately 70% of our triggers were reconstructed to give good dimuon pairs. A typical high mass event is shown schematically in Fig. 2. The hits in the PWC's and the hodoscopes are shown, along with the reconstructed muon trajectories.

3. Acceptance and Systematics.

As a check on background produced by random dimuon coincidences, a scaled sample of events with one arm delayed by two rf buckets with respect to the other was also recorded. These could be compared with the like sign events taken along with the opposite sign events. To make the comparison precise, one of the like sign events was reflected in the horizontal mid-plane before calculating the mass. This corrects for the difference of the acceptance of the opposite and like sign pairs. The reflected like sign data, along with the opposite sign raw data for the high mass trigger is shown in Fig. 3. As can be seen, the background from accidentals is typically 1% or less in the high mass region.

In Fig. 4 we show the acceptance of the apparatus as a function of q^2

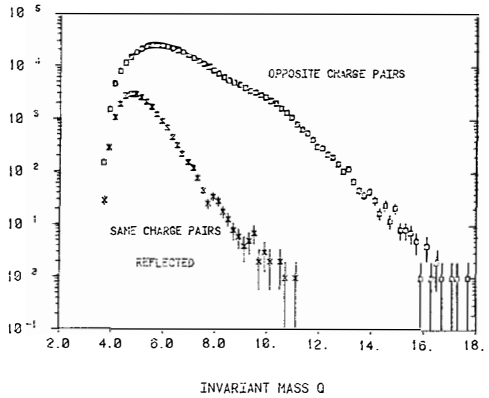

Fig. 3. Accidental Rate. This is a plot of our raw high mass data and the accidental data as evidenced by the like sign pairs.

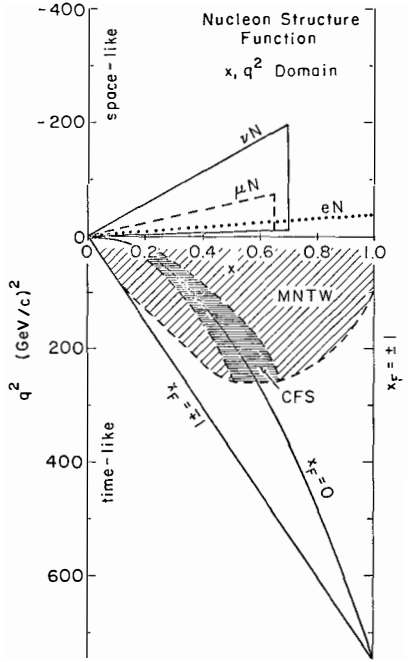

Fig. 4. Apparatus Acceptance. The acceptance of the apparatus is shown for Bjorken x and q^2. Also noted are the acceptances of the deep inelastic lepton scattering experiments in the space-like region and the CFS acceptance at 400 GeV. The dashed boundary is the limit of useful statistics.

versus Bjorken x of the partons. The dashed boundary is not a geometrical cut-off but is determined by the limit of useful statistics. Also noted is the region covered by the CFS group at 400 GeV and by the deep inelastic lepton scattering experiments in the space-like domain.

In order to correct the data for the systematics of the apparatus acceptance and the interaction of muons in iron, a Monte Carlo program was used that simulated the effects, including the fluctuations, of multiple scattering, knock-on electrons, bremmstrahlung, pair production and finite radiative corrections.[3] The finite resolution of the PWC's was also included.

In Fig. 5 we show the corrected dimuon mass spectrum for dimuon events with Feynman x from 0 to 0.2. The three curves labeled (a), (b), and (c) are acceptance functions for the different triggers used and reference the scale at the right. For (a) the two arms were together, for (b) the two arms were separated by 18 mr and for (c) the high mass wedge counter trigger was satisfied as well as the matrix logic conditions. These acceptances are affected by the geometry as well as the resolution because muon pairs can scatter into the acceptance. The dimuon spectra resulting from the three different triggers after correction agreed to better than 5% in the two regions of overlap. A small correction for random coincidences has been made from the like-sign pairs $\mu^+\mu^+ + \mu^-\mu^-$ and for muons produced by pions in the target. The inset shows the events in the Upsilon region on a linear scale after a subtraction of the continuum is made. The shape agrees very well with our Monte Carlo results.

4. Sea Quark Distribution.

To find the sea quark distribution we use the events from the region shown in Fig. 6. These are the events shown in Fig. 5 above 5 GeV in mass and excluding the Upsilon region. Using the value of $F_2^p(x,q^2)$ found in deep inelastic lepton scattering[4], we fit our spectrum with the function

$$C_1F_2^p(x_1,q^2)S(x_2)+C_2S(x_1)F_2^p(x_2,q^2)+C_3S(x_1)S(x_2)$$

where C_1, C_2 and C_3 are known functions of x_1 and x_2 and S(x) specifies the sea quark distribution. We have used the parameterization of F_2^p given by T. Kirk.[5] For the q^2 evolution we have assumed that $q^2 = m^2$ where m is the dimuon mass, and have ignored the sign change. F_2^n was obtained from the SLAC deep inelastic electron scattering[6] and we have assumed that $F_2^n/F_2^p = .807 - .535x$ is independent of q^2.

The $\bar{u}$ $\bar{d}$, $\bar{s}$ and s sea quark distributions have been parameterized in two ways:

A. symmetric sea: $x\bar{d} = x\bar{u} = 2xs = 2x\bar{s} = a(1-x)^b$

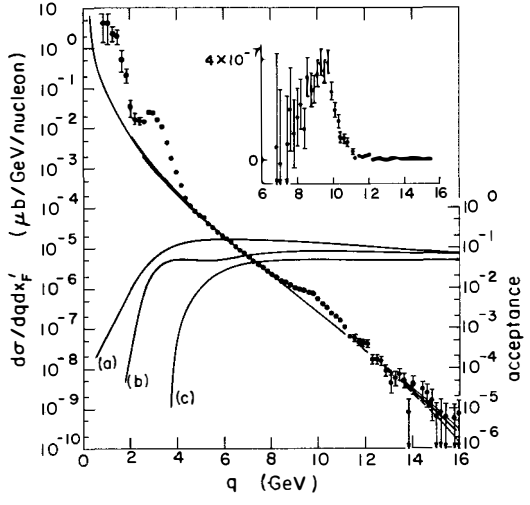

Fig. 5. Dimuon Production Cross Section. This shows the dimuon cross section for events in the region of $0<x_F'<0.2$ versus mass, q. Mass dependent systematic errors are indicated by the spread in the fitted curve and are in addition to an 11% overall error. The fit is the result of the asymmetric sea determination. The curves labeled (a), (b), and (c) are the acceptances for the three triggers used and reference the scale to the right.

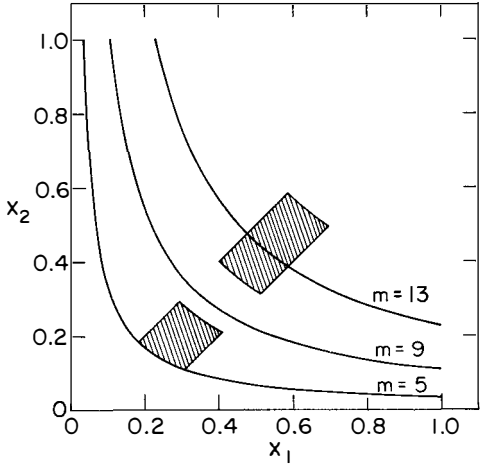

Fig. 6. Sea Quark Fit. x_1 and x_2 are the Bjorken x values of the beam and target partons, respectively. The shaded area is the region from which the sea quark distributions were determined.

B. Asymmetric sea: $x\bar{d} = a(1-x)^b$

$$x\bar{u} + (1-x)^{2.5} x\bar{d}$$

$$xs = x\bar{s} = (x\bar{u}+x\bar{d})/4$$

All higher mass quark flavors are neglected. The asymmetric form is suggested by the results of the CFS group.[7)]

The results of a best fit to the data in Fig. 6 for the parameters a and b are given in the following table.

	A	B
a	.46±.03±.06	.50±.03±.06
b	8.2±.2±.3	7.4±.2±.3

where the first error is statistical and the second an estimate of the systematics. In Fig. 5, the solid curve is the fit using the asymmetric sea and has a chi-square of 35 for 35 degrees of freedom. The broadening of the curve is a measure of the systematics. These are largely due to the uncertainty of the extent of the dimuon production from secondary particles. There is also an overall 11% uncertainty in the normalization of our data.

We emphasize that the q^2 dependence of the sea cannot be obtained from this fit, since each point, x, for the sea quark distribution is essentially measured at a single value of q^2. If the sea quark distributions are compared with those obtained by the CDHS collaboration[8)] (although these were at lower q^2), we find a larger value by a factor of 1.6±0.3 in the region of overlap. This ratio is customarily called the K factor, and is somewhat smaller than that obtained from the pion data,[9)] but the difference may be due to scale breaking.

5. Test of Drell-Yan

Having obtained these sea quark distributions we can then compare the predictions of the Drell-Yan model with the cross section observed in the remainder of phase space detected by our apparatus. To systematically note the edge of phase space we use the variable $x_F' = x_F/(1-\tau)$ where $\tau = m^2/s$. That is, Feynman x is scaled by the maximum possible value for a given mass. In Fig. 7 we show on a linear scale the cross section prediction of the Drell-Yan model vs. x_F' (compared with the data) for dimuon masses in the region of 11.5 GeV. The normalization of the curve comes from the fit in the x_F' region of .0 to 0.2 and the shape depends upon the Drell-Yan model. In Fig. 8 we show the results on a logarithmic scale for 5 different mass bins. The curves show excellent agreement with the data. The chi-square per degree of freedom are as follows:

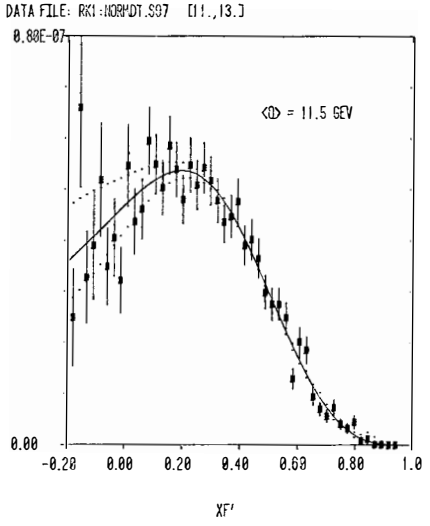

Fig. 7. Test of Drell-Yan. This shows a comparison of the cross section predicted by the Drell-Yan model and our data in the 11.5 GeV mass region. The sea quark distribution was obtained from the asymmetric fit. The dotted curve is a measure of our systematic uncertainty.

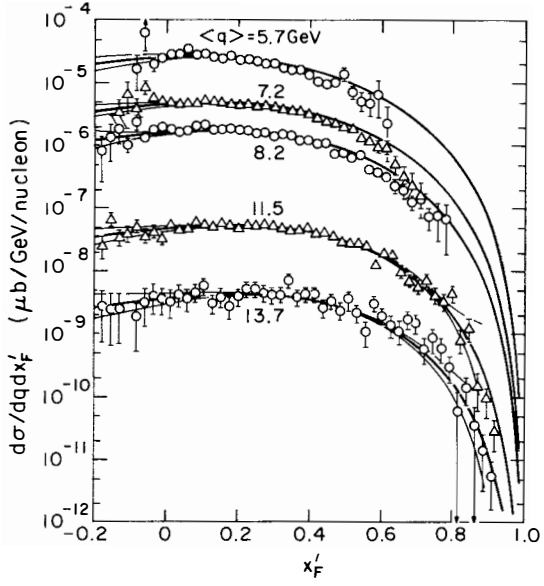

Fig. 8. Test of Drell-Yan. This shows a comparison of the Drell-Yan model predictions for five different mass bins with our data. The lack of events at low mass and large x_F' is due to limited statistics.

mass	chi-square	degree of freedom
5.7 GeV	93.5	30
7.2	73.7	36
8.2	116.5	41
11.5	74.5	47
13.7	37.3	46

The cut-off in the data at large x_F' and low mass is due to the poor acceptance in this region by the high mass trigger and the limited statistics obtained with the low mass trigger. The poorer fits at the lower masses could be due to our parameterization of F_2, a K factor variation or scale breaking in the sea. Scale breaking is expected and could be included to improve the fit to the data.

6. Upsilon Production

The production mechanism for the resonances observed in hadron production of dimuons is as yet uncertain and several mechanisms have been suggested[10]. The ratio of the Upsilon to the continuum as a function of x_F' is clearly sensitive to the production mechanism and a ratio avoids errors introduced by absolute normalization. For example, if the production were mainly due to quark-antiquark annihilation, then the ratio would be expected to be approximately constant for different Feynman x values. Small differences in the behavior of the up and down quark structure functions would prevent the ratio from being precisely constant. On the other hand, a substantial component of gluon production would cause the ratio to decrease with Feynman x. Given the gluon structure function different models can be tested or given a model, the gluon structure can be constrained. We show the ratio of the Upsilon family to continuum production vs. x_F' in Fig. 9.

The ratio plotted in Fig. 9 is given by

$$R = (d\sigma(\Upsilon)/dx_F')/(d^2\sigma(C)/dm dx_F')$$

in units of GeV. The data has not been corrected for absorption in the tungsten nucleus, but this is expected to be small. We have also assumed that the decay angular distribution for the Upsilon family is isotropic. Our results agree well with the point obtained by the CFS group shown on the plot. The decrease in the ratio as a function of x_F is characteristic of substantial production by gluons.

6. P_t Dependence

It is now clear that the Drell-Yan process involves a sizeable amount of gluon radiation. This radiation may be responsible for a large fraction of the

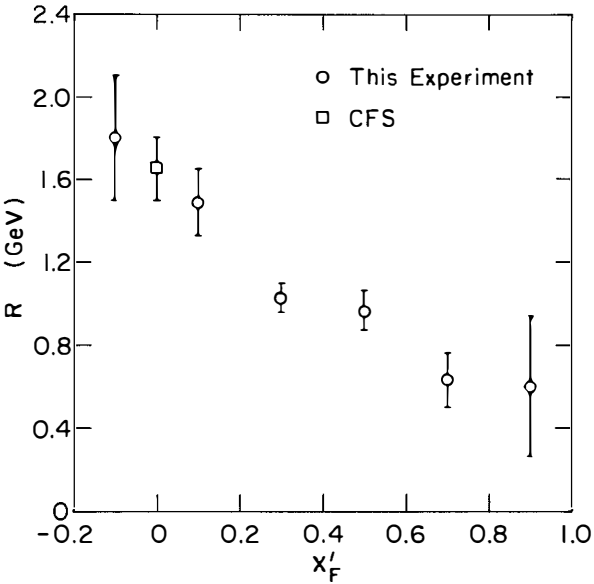

Fig. 9. Upsilon to Continuum Ratio. This shows the ratio of the Upsilon family production cross section to the continuum cross section in the Upsilon region as a function of x'_F.

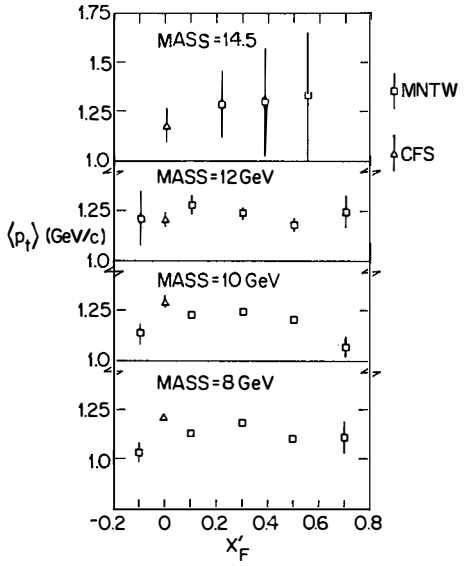

Fig. 10. Average P_t. Plotted here is the average P_t of the dimuon pairs versus x'_F for four mass intervals. No significant decrease in the average P_t with increasing x'_F is indicated, although a slight increase with increasing mass is apparent.

transverse momentum carried by the dimuon pairs. In Fig. 10 we show the mean value of the dimuon P_t as a function of x_F' for several mass bins. The data indicate a mean value that is independent of x_F' and slowly increases with mass. Hopefully QCD will be able to explain the precise nature of this behavior, although the predicted decrease in mean P_t with Feynman x is not observed.[11]

7. Summary

We can summarize our results as follows: We have obtained sea quark structure functions similar to those obtained in other processes but with a K factor of 1.6±0.3. Using the Drell-Yan model, these structure functions are used to predict the behavior of the cross sections for a large range of mass and Feynman x. The agreement with our data is very good.

We have found that the ratio of the Upsilon production to continuum decreases substantially with Feynman x, which indicates a significant amount of the production involves gluons.

The average value of P_t for the continuum is found to be large and independent of Feynman x. The average value does show a small increase with increasing dimuon mass.

References

1) S. W. Herb et al., Phys. Rev. Lett. 39, 252(1977).
2) D. A. Garelick et al., Phys. Rev. D18, 945 (1978).
3) A. Soni, Phys. Rev. D8, 2264 (1973).
4) B. A. Gordon et al., Phys. Rev. D20, 2645 (1979).
5) T. B. W. Kirk, Fermilab Report Number TM-791 (1978).
6) A. Bodek et al., Phys. Rev. D20, 1471 (1979).
7) A. S. Ito et al., FERMILAB-Pub-80/19-EXP(1980).
8) J. G. H. de Groot et al., Zeitschrift fur Physik C1, 143 (1979).
9) For a summary see, for example, G. Matthiae CERN-EP/80-183.
10) J. F. Owens and E. Reya, Phys. Rev. D17, 3003 (1978) and R. Rückl at this conference.
11) F. Halzen and D. M. Scott, Phys. Rev. Lett. 40, 1117 (1978).